

SITE PERFORMANCE TEST EVALUATION FOR GAS TURBINE AND ELECTRIC MOTOR DRIVEN COMPRESSORS

by

Rainer Kurz

Manager of Systems Analysis and Field Testing

Solar Turbines Incorporated

San Diego, California

and

Klaus Brun

Principal Engineer

Southwest Research Institute

San Antonio, Texas



Dr. Rainer Kurz is Manager of Systems Analysis and Field Testing for Solar Turbines, Incorporated, in San Diego, California. His organization is responsible for predicting gas compressor and gas turbine performance, for conducting application studies, and for field performance tests on gas compressor and generator packages.

Dr. Kurz attended the University of the Federal Armed Forces in Hamburg, Germany, where he received the degree of a Dipl.-Ing. in 1984 and the degree of a Dr.-Ing. in 1991. He has authored numerous publications in the field of turbomachinery and fluid dynamics, is an ASME Fellow, and a member of the Turbomachinery Symposium Advisory Committee.



Dr. Klaus Brun is a Principal Engineer at Southwest Research Institute, Mechanical and Materials Engineering Division, in San Antonio, Texas. His experience includes positions in business development, project management, engineering, and marketing at Solar Turbines, General Electric, and ALSTOM Power. He is the inventor of the Single Wheel Radial Flow Gas Turbine and co-inventor of the Planetary Gear Mounted Auxiliary Power

Turbine. He has authored over 30 papers on turbomachinery, given numerous technical lectures and tutorials, and published a textbook on Gas Turbine Theory. He is the incoming Chair of the ASME-IGTI Oil & Gas Applications Committee, a member of the Gas Turbine Users Symposium Advisory Committee, and a past member of the Electric Power and Coal-Gen Steering Committees.

Dr. Brun received his Ph.D. and M.Sc. degrees (Mechanical and Aerospace Engineering, 1995, 1992) from the University of Virginia, and a B.Sc. degree (Aerospace Engineering, 1990) from the University of Florida.

ABSTRACT

Field testing of compressor packages driven by gas turbines or electric motors requires the accurate determination of efficiency, flow, head, and power in sometimes less than ideal working environments. This paper discusses field performance testing of

centrifugal compressors and measurement uncertainties one can expect when following appropriate test guidelines. The primary focus is on compressor performance for applications where the compressor is controlled by speed variation. Special consideration will be given to testing of compressors with two sections and multicompressor trains. The paper addresses the issues of planning and organization of field tests and necessary instrumentation, but primarily focuses on data reduction, data correction, test uncertainty, and the interpretation of test data.

INTRODUCTION

Centrifugal gas compressors are used in many applications in the oil and gas industry, such as in pipelines, for gas gathering, gas reinjection, gas lift, gas storage, in onshore as well as offshore environments. The predominant driver for these compressors is two shaft gas turbines, and, to some extent, variable speed electric motors. Both types of drivers have in common that the speed of the compressor can be varied easily over a large range. To some extent, variable speed electric motors are used in similar tasks. Performance testing of compressor packages is becoming increasingly frequent because economic pressures demand that the efficiency, power, fuel flow, capacity, and head of an installation be verified to assure a project's return on investment. Test results may have significant financial implications for the compressor and gas turbine manufacturers and their customers. They may be the basis of future decisions on plant modifications or extensions, or may serve as baseline data for monitoring purposes. Field tests also provide the operator and the equipment manufacturers with information complementary to the data collected during factory testing. Thus, for the end user and the manufacturer, an accurate determination of the package field performance is critical. This paper discusses problems and challenges related to the field performance testing of gas turbine or electric motor driven, variable speed compressor sets.

Insights from over 100 field performance tests on centrifugal compressors are described. Such field tests provide the user with valuable operation and maintenance data and the manufacturer with information complementary to the data gathered through factory testing.

This paper also describes in detail how raw test data (i.e., measured pressures, temperatures, flows, and speeds) are converted into meaningful data that can be used for evaluating the performance of a gas turbine or a gas compressor. Details on instrumentation will not be provided by this paper, but can be found elsewhere (Kurz, et al., 1999). The data reduction is explained based on the basic relationships of pressure, temperature, flow, and head, as well as the operational characteristics of

centrifugal gas compressors, with special consideration of test uncertainties. Methods of data correction are explained. A few remarks on general procedures, valid for any type of test, including the application of test uncertainties are included.

Assume a performance test has just been concluded and columns of pressures, temperatures, and speeds have been measured. Fuel and process gas compositions are known. The test was conducted using a reasonably accurate test protocol (ASME PTC 10, 1997; Kurz, et al., 1999). The test was conducted to gain information about the performance of the gas turbine driven centrifugal compressor set. The question is now (actually, this question should have been asked prior to the test), what to do with all that data? In this paper, the authors want to review methods to reduce the raw test data to information about the performance of the compression system.

SYSTEM DESCRIPTION AND PERFORMANCE MAPS

The system discussed consists of a two-shaft gas turbine or a variable speed electric motor driving one or more centrifugal compressors (Figure 1). Possibly, a gearbox is used between the driver and the driven equipment or between compressors. Figure 2 outlines the test data taken on a single compressor:

- Suction pressure and temperature
- Discharge pressure and temperature
- Flow and gas composition
- Speed

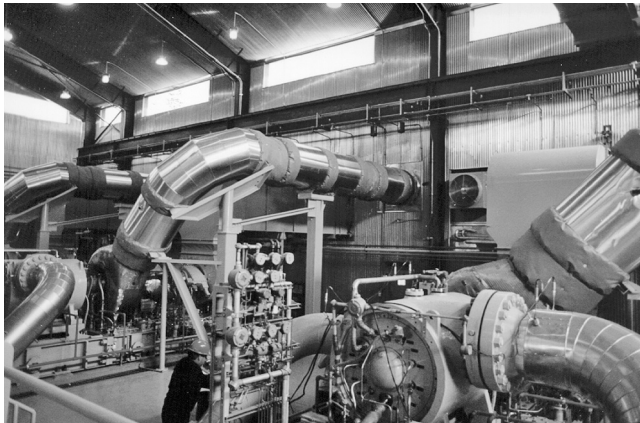


Figure 1. Compressor Station with Three Gas Turbine Driven Centrifugal Compressors.

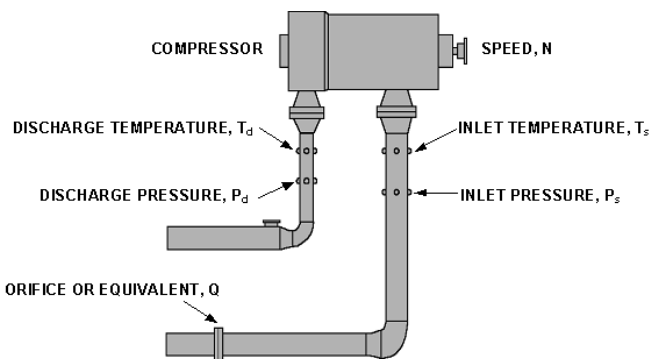


Figure 2. Test Data for Centrifugal Compressors.

Usually, the manufacturer of the gas compressor provides a set of performance maps for the equipment (Figure 3).

For the compressor, there are maps showing suction or discharge pressure over the standard flow for various operating speeds and

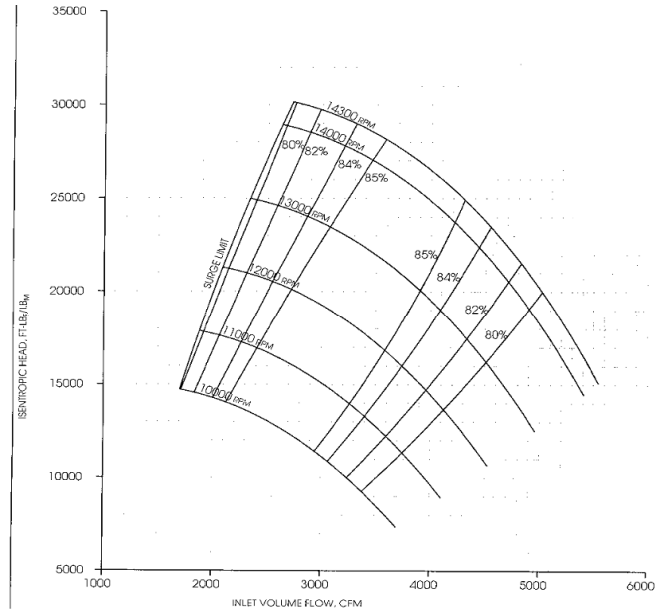


Figure 3. Typical Gas Compressor Performance Map.

maps that show isentropic or polytropic head over actual compressor inlet flow, also for various operating speeds. For the purpose of this test data evaluation, only the head-versus-actual flow maps are useful because the pressure-versus-flow maps are only valid if the compressor suction conditions (pressure, temperature, gas composition) are exactly the same as indicated on the map.

The authors will use these maps, which are based on the manufacturer's predictions of the equipment performance, to compare their test data against.

DATA REDUCTION—HOW TO GET POWER, FLOW, AND EFFICIENCY FROM ALL THESE PRESSURES AND TEMPERATURES

Single Gas Compressor

The flow through the compressor (as well as the gas turbine fuel flow) has been measured using one of several possible flow measuring devices. If the device is a flow orifice, the relationship between the flow and the measured temperatures and pressures is as follows:

$$W = C \cdot E \cdot \frac{\pi}{4} \cdot d^2 \sqrt{2 \cdot \Delta p \cdot \rho_1} \quad (1)$$

C and E are discharge coefficients and the velocity approach factor, respectively, and d is the orifice throat diameter. The coefficients can be determined either from the orifice manufacturer's data sheets or from such codes as ASME PTC 19.5 (1971) or ISO 5167 (1980).

Other devices (venturi, pitot-type probes, etc.) have formally similar relationships between the flow and the measured pressures and temperatures. Devices that do not use the pressure differentials, such as turbine flowmeters, ultrasonic flowmeters, and coriolis flowmeters will be supplied by their respective manufacturers with appropriate methods to calculate actual flow and standard flow or mass flow. It must be noted that, while the standard flow through the flow measuring device and the compressor are identical (as long as no leaks or flow divisions are present), the actual flow will be different because the pressure and temperature at the compressor nozzle will be different from the actual flow through the flow measuring device. For now, one can state that any flow measuring device will provide one with either the standard flow (SQ) or the mass flow (W). (Standard conditions can be 60°F and 14.70 psia, 60°F and 14.73 psia, or 15°C (59°F)

and 760 mm Hg (14.7 psia). Many countries use “normal” conditions, such as 0°C (273.15 K, 32°F) and 1013.25 mbar (1 atm, 14.7 psia.)

The knowledge of pressure and temperature at the compressor inlet nozzle enables us to calculate the actual flow (Q_s) with:

$$Q_s = \frac{W}{\rho_s} \quad \text{or} \quad Q_s = \frac{SQ \cdot \rho_{std}}{\rho_s} \quad (2)$$

The density in the above equations has to be determined using an equation of state. The general relationship is:

$$\rho = \frac{P}{Z(p, T) \cdot R \cdot T} \quad (3)$$

The compressor head (H) can be determined from the measurement of suction and discharge pressure and temperature. The relationship between the pressure, temperature, and the enthalpy (h) is defined by the equations of state described below.

By using the equations of state, the relevant enthalpies for the suction, the discharge, and the isentropic discharge state can be computed. The isentropic head (H^*) is:

$$H^* = h(p_d, \Delta s = 0) - h(p_s, T_s) \quad (4)$$

The actual head H is:

$$H = h(p_d, T_d) - h(p_s, T_s) \quad (5)$$

[In US units, the enthalpy difference (Btu/lb) has to be multiplied by the “mechanical equivalent of heat” (778.3 ft lb/Btu) to get the head (ft lb/lb)].

The isentropic and polytropic efficiencies then become:

$$\eta^* = \frac{H^*}{H} \quad \eta^p = \frac{H^p}{H} \quad (6)$$

It should be noted that the polytropic efficiency is defined similarly to the isentropic efficiency, using the polytropic process instead of the isentropic process for comparison. The actual head, which determines the absorbed power, is not affected by the selection of the polytropic or isentropic process. However, the isentropic head is unambiguously defined by the user’s process data (i.e., gas composition, suction pressure and temperature, discharge pressure), while the polytropic head for full definition additionally requires the compressor efficiency or the discharge temperature.

The task of gas compression is to bring gas from a certain suction pressure to a higher discharge pressure by means of mechanical work. The actual compression process is often compared to one of two ideal processes.

The compression process is isentropic if the process is frictionless and no heat is added to or removed from the gas during compression. With these assumptions, the entropy of the gas does not change during the compression process, and the process is reversible. Because there is no heat transfer across the system boundaries, the process is often referred to as reversible adiabatic.

The polytropic compression process is like the isentropic cycle reversible, but it is not adiabatic. It can be described as an infinite number of isentropic steps, each interrupted by isobaric heat transfer. This heat addition allows the process to yield the same discharge temperature as the real process.

Either process can be used for the definition of the operating point and the efficiency of the compressor. It should be noted that the absorbed compressor power is not impacted by this choice, because it solely depends on the actual head. Since the site test will in many instances be performed at conditions very similar to the design point, the isentropic definition has the advantage that the

isentropic head (and thus the operating point) is fully defined by the process conditions (gas, suction and discharge pressure, and suction temperature), while the polytropic head additionally depends on the compressor efficiency, which in itself is the subject of the test.

The comparison of the actual process with a polytropic process, as opposed to an isentropic process, has the advantage that the efficiency for an aerodynamically similar point is less dependent on the actual pressure ratio. However, it has the disadvantage that the polytropic head for a given set of operating conditions depends on the efficiency of the compressor, while the isentropic head does not.

With the flow from above, the aerodynamic or gas power of the compressor, then, is determined to be:

$$P_g = \rho_1 Q_1 H = \frac{P_1}{Z_1 R T_1} Q_1 H \quad (7)$$

The absorbed power (“brake power”) P is calculated by dividing the internal power (gas power) by the mechanical efficiency η_m :

$$P = P_g / \eta_m = \frac{W}{\eta_m} [h(p_{t2}, T_{t2}) - h(p_{t1}, T_{t1})] = \frac{W}{\eta_m} \cdot \frac{H^*}{\eta^*} \quad (8)$$

After considering the mechanical efficiency (η_m) (typically around 98 to 99 percent), which accounts for bearing, seal, and windage losses, the absorbed (or “brake”) power (P) of the compressor becomes:

$$P = \frac{P_g}{\eta_m} \quad (9)$$

Related to measurements of head and flow is also the determination of the surge point or the surge line. The main challenge lies in the fact that steady-state conditions are required for any of the measurements discussed herein. By definition, surge is a nonsteady condition. Even close to surge, most readings start to fluctuate. The determination of flow at surge is, thus, much more inaccurate than measurements further away from surge.

The method to use increased vibration levels as an indication of surge, or incipient surge, is even more inaccurate because the increased vibration levels might be generated by the onset of rotating stall (which is by no means identical with the onset of surge) or other conditions.

Equations of State

The aerothermodynamic performance of a gas compressor is defined by enthalpy and entropy differences, so an additional problem arises: enthalpies and entropies cannot be measured directly, but have to be calculated by the use of an equation of state (EOS). The state of any fluid consisting of known components can be described by any given pair of its pressure, specific volume, and temperature. Equations of state approximate these relationships. The equations can also be used to calculate enthalpy and entropy from the condition of a gas given by a pressure and a temperature (Baehr, 1981).

The simplest equation of state is the equation for a perfect gas:

$$pv = p / \rho = RT \quad (10)$$

Real gases and in particular gas mixtures, however, display complex relationships between pressure, volume, and temperature (p-v-T). EOS use semiempirical equations to describe these relationships, in particular the deviations from perfect gas behavior:

$$\frac{P}{\rho} = Z(p, T) \cdot R \cdot T \quad (11)$$

They also allow for the calculation of properties that are derived from the p-v-T relationships, such as enthalpy (h) and entropy (s).

Because EOS are semiempirical, they might be optimized for certain facets of the gas behavior, such as liquid-vapor equilibria and not necessarily for the typical range of temperatures and pressures in various compression applications. Because different EOS will yield different values for density, enthalpies, and entropies, the EOS has to be agreed upon before the test.

Usually, it is not possible to select a “most accurate” EOS to predict enthalpy differences, since there usually is no “calibration normal” to test against. All the frequently used EOS (RK, BWR, BWRS, LKP, RKS, PR) show reasonably correct enthalpies. It is just not possible to decide which of them is more accurate for a given application (Kumar, et al., 1999). Therefore, it is recommended to use the EOS for test data reduction that was also used for the performance prediction. This procedure is also recommended in VDI 2045 (1993) to avoid additional test uncertainties.

Most equations of state used in gas compression applications are either cubic equations (RK and its derivatives SRK and PR), and Benedict-Webb-Rubin derivatives (BWR, BWRS, LKP). Beinecke and Luedtke (1983) have conducted thorough evaluations on the accuracy of the Lee-Kesler-Ploecker (LKP) method, the Benedict-Webb-Rubin-Starling (BWRS) method, and the Soave-Redlich-Kwong (SRK) method. All of the EOS mentioned can predict the properties of hydrocarbon mixtures quite accurately over a wide range of pressures. Still, deviations of 0.5 to 2.5 percent and greater in the values for gas density are common. Even more important than the compressibility factor is the calculation of the enthalpy and entropy using the EOS. Because derivatives of the EOS have to be used to perform these calculations (Poling, et al., 2001), the deviations can be even larger than for the compressibility factor.

Figure 4 shows the effect of different EOS on the results for a given set of typical test data. The isentropic efficiency was calculated based on four equations of state, using the Redlich-Kwong equation as a reference. Depending on the pressure ratio, the four different EOS deliver four different results for the same measured conditions. For the calculations in the example, the following conditions were used. Suction condition was always at $T_1 = 20^\circ\text{C}$ (68°F) and $p_1 = 50$ bar (725 psia). The gas was compressed to varying end pressures (p_2) with T_2 chosen such that the reference EOS (RK) yields 80 percent efficiency. The results are shown in Figure 4. Differences as high as 2 percent exist among the EOS models. Clearly, it cannot be concluded that a certain EOS will always lead to higher efficiency than other EOS.

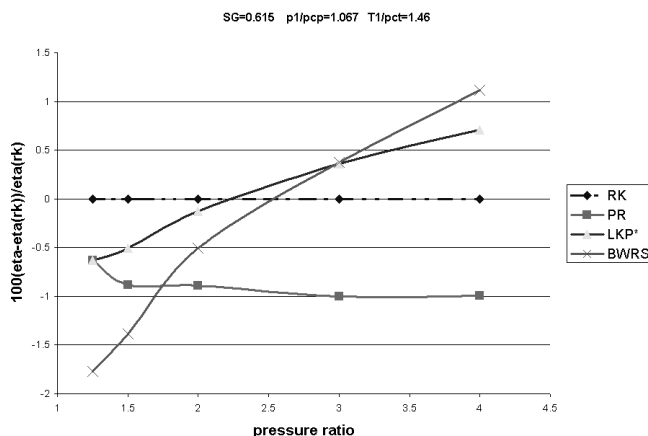


Figure 4. Isentropic Efficiency Differences among EOS for a Natural Gas Mixture (when $p_1 = 50$ bar (725 psia), $T_1 = 20^\circ\text{C}$ (68°F) and varying p_2 , T_2 chosen to give $\eta = 80$ percent for RK EOS). (Courtesy Kumar, et al., 1999)

EOS may differ from program to program because sometimes different mixing rules are used, different interaction parameters between the gases are assumed, or a different treatment of the ideal

gas portion in the EOS is used. Poling, et al. (2001), give an overview of the theory behind equation of state procedures.

Considerations for Trains with Multiple Compressors

In trains with multiple compressors, each compressor is treated individually, both as far as pressure, temperature, flow measurements, and gas compositions are concerned, but also with regards to the design points. The latter requirement is due to the fact that site conditions rarely allow both (or all three) compressors to operate at their respective design points at the same time. Therefore, their power consumption has to be determined individually, and later added up. If all compressors are completely instrumented, the power requirement of the train (and thus the power generated by the driver) can be determined.

Considerations for Compressors with Multiple Sections

The particular challenge for compressors with multiple sections is to correctly separate the absorbed power for the individual sections. The difficulty arises from the fact that there can be significant mass transfer (due to leakage across the division wall) and possibly heat transfer (again, across the division wall) from section to section. It should be noted that the measurement of the overall power consumption of the compressor is not affected by these internal transfers. However, they can lead to observed efficiencies that are too high for the first section, and too low for the second section, or vice versa. For compressors with multiple sections, the absorbed power is:

$$P = \frac{1}{\eta_m} \cdot \sum_{i=1}^n P_{G,Section_i} \quad (12)$$

This relationship is valid, as long as all flows in and out of the system are considered. Internal leakage does not affect it.

The main difficulty in the determination of the performance of individual sections lies in the fact that the interstage leakage has an impact on the observed section performance. The interstage leakage can be determined by either:

- Measuring the flow into the first section inlet, the first section discharge, and the second section inlet
- Measuring the flow into the first section inlet, measuring the flow into the second section inlet, and estimating the leakage flow based on theoretical considerations or factory test data.

Either method will yield the inlet flow used in the calculations above.

For machines in back-to-back configuration (Figure 5), the measured inlet temperatures and pressures will be used to calculate actual inlet flow and the enthalpies of the gas flowing into the respective sections. To calculate the enthalpy rise over the section, the measured discharge pressures can be used. The measured discharge temperatures will be corrected for the effect of the division wall leakage by:

$$H_2^I = \frac{1}{W_1^I} \left[H_{2,meas}^I (W_1^I + W_L) - W_L H_L \right] \quad (13)$$

$$T_2^I = f(H_2^I, p_2, gas)$$

This procedure yields the suction flow, suction temperatures, and discharge temperatures for the calculation of section head, section efficiency, and section absorbed power as outlined in Equations (2) through (9). The isentropic head of either section is not affected by the leakage, while the discharge temperature necessary for the calculation of the polytropic section head (and the section efficiency) can be derived from the calculation above. The method described above assumes that section I has a lower discharge pressure than section II, and therefore the leakage is from the section II to section I.

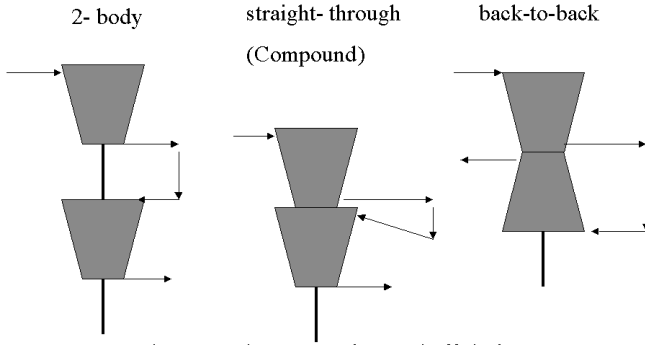


Figure 5. Configurations for High Pressure Ratio Compressor Trains—Two-Body Tandem, Straight Through (Compound) Compressor, Back-to-Back Compressor. Usually, Intercoolers Are Used to Reduce the Exit Temperature from the First Section to a Lower Inlet Temperature into the Second Section.

For compound machines (Figure 5), the leakage over the division wall can normally be neglected because the pressure differential is usually only due to pressure loss in the intercooler and the piping.

Using either procedure, the combined absorbed power of the sections with the added mechanical losses yields the shaft power of the compressor.

TEST CONDITIONS VERSUS REFERENCE CONDITIONS—COMPARING TEST DATA

Usually, the operating points for the test are determined by the facility and the test may not be conducted at some desired condition. Also, when test data are taken over time for condition monitoring purposes, the data are taken for different operating conditions. Therefore, there is a need to compare data taken or predicted at different conditions. Note that the gas compressor test may serve several purposes, for example:

- To determine the compressor performance
- To load the gas turbine to full load to determine the gas turbine output and full-load heat rate
- To verify the performance of the entire train

For site tests it is always of advantage to compare the test data with other, redundant measurements. For example, the gas turbine driver full load performance may be known from a recent factory test. If the compressor can be operated with the engine running at full load, the compressor shaft power equals the engine full load output. This engine performance can then be corrected to factory test conditions (Kurz, et al., 1999), and should be reasonably close to the factory test results. If the gas turbine fuel flow can be measured, a similar comparison can be made for the heat rate. If the results from the site test and the factory test are reasonably close, the confidence in the site test results is improved. Otherwise, reasons for the discrepancy should be determined.

Similarity Conditions for Gas Compressors

The goal of a site test should be to create conditions that are as close as possible to the original design conditions. The approach to a site test is thus different from the approach to a factory test, where a number of correction methods are used to correct performance for vastly different conditions.

To compare test data for a centrifugal compressor, it is very useful to use nondimensional parameters for head and flow. Efficiency is already a nondimensional value.

Using the Flow Coefficient:

$$\phi = \frac{Q_s}{\frac{\pi}{4} D_{1,tip}^2 u} = \frac{Q_s}{\frac{\pi^2}{4} D_{1,tip}^3 N} \quad (14)$$

and Head Coefficient (isentropic or polytropic):

$$\psi^* = \frac{H^*}{\frac{u^2}{2}} = \frac{2H^*}{(\pi D_{1,tip} N)^2} \quad \psi^p = \frac{H^p}{\frac{u^2}{2}} = \frac{2H^p}{(\pi D_{1,tip} N)^2} \quad (15)$$

eliminates the requirement to test the compressor precisely at the same speed as predicted. It allows one to compare data taken at (somewhat) different speeds. (The same can be accomplished by using the term Q/N and H/N^2 . However, these parameters are not nondimensional.) This is because as long as ϕ and ψ (as well as some other parameters described below) are maintained, the aerodynamics of the compressor are not impacted by the different operating condition. Figure 6 shows a typical, nondimensional compressor map.

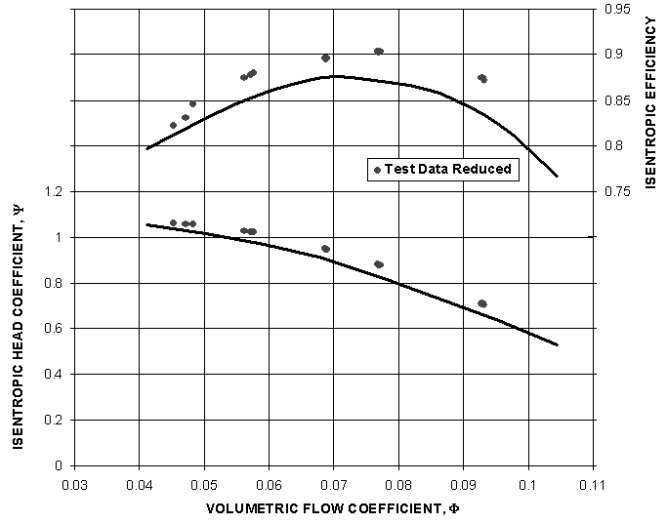


Figure 6. Nondimensional Compressor Map.

The other parameters that need to be maintained to accomplish similarity (although with some possible deviations) are:

Machine Mach Number:

$$Ma_u = \frac{u}{\sqrt{k_s Z_s R T_s}} = \frac{\pi D_{tip} N}{\sqrt{k_s Z_s R T_s}} \quad (16)$$

Machine Reynolds Number:

$$Re_u = \frac{\pi D_{tip} N b_{tip}}{v_s} \quad (17)$$

Isentropic Exponent:

$$k = \left(\frac{v \delta p}{p \delta v} \right) \quad (18)$$

Volume Flow Ratios:

$$\left(Q_s / Q_d \right)_t = \left(Q_s / Q_d \right)_a \quad (19)$$

Typically, only some of the similarity parameters can be brought into accordance with the desired acceptance criteria, especially when the gas composition during the test is different from the design gas. The most important parameters are head and flow coefficients and the machine Mach number. Maintaining the volume/flow ratios is also desirable.

When keeping the flow coefficient the same as for the design case, the velocity triangles at the inlet into the first stage remain the same. Together with the head coefficient, this defines a singular operating point of the compressor, as long as the fan law remains applicable. If the volume flow ratios between inlet and outlet are kept the same as for the design case, the velocity triangle at the outlet of the compressor also will be the same. Generally, this requirement involves keeping the same machine Mach number and the same average isentropic exponents over the machine (at least approximately).

For most applications, the Reynolds number similarity is of lesser importance because the Reynolds numbers are relatively high and clearly in the turbulent flow regime. Additionally, the loss generation in centrifugal compressors is only partially due to skin friction effects, i.e., due to effects that are primarily governed by Reynolds numbers.

Certain deviations between design and test case for these parameters are acceptable and unavoidable. In general, as long as the deviations between test and design stay within limits as described in ASME PTC 10 (1997), or in VDI 2045 (1993), a simple correction based on the fan law can be used. Namely, the test point must be at the same combination of ϕ and ψ [Equations (14) and (15)] as the design point. The limitations of the fan law are also discussed by Brown (1991). Pipeline compressors, with usually only one or two impellers per body, are typically less sensitive to deviations from the above parameters (Figure 7). Multistage machines show more sensitivity.

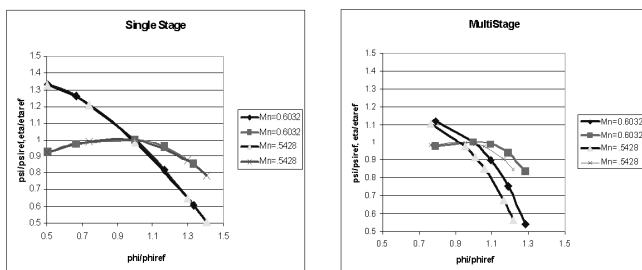


Figure 7. Effect of Machine Mach Number Variations on Gas Compressor Performance. (Courtesy, Kurz and Fozi, 2002)

If the test conditions are considerably different from the design conditions, for example outside of the limits established in ASME PTC 10 (1997), or, in more general terms, when the fan law is no longer applicable, easy corrections for Mach numbers and volume/flow ratios are not available. Often, the design programs of the compressor manufacturer can be used to recalculate the compressor performance for the changed design conditions, which are new curves for head coefficient versus flow coefficient, and efficiency versus flow coefficient are generated for the new conditions.

ASME PTC 10 (1997) assumes for a Type 1 test that the test gas is almost identical to the gas for the specified acceptance conditions. In a field test, the gas composition cannot be controlled by the equipment manufacturer and the test gas might deviate from the specified gas. In case the actual test gas deviates significantly, the compressor performance can be recalculated for the actual test gas.

Deviations also occur if the gas was specified incompletely, for example, by only defining the specific gravity rather than a full gas composition.

TEST UNCERTAINTIES

Test uncertainties need to be clearly distinguished from building tolerances. Building tolerances cover the inevitable manufacturing tolerances and the uncertainties of the performance predictions. The actual machine that is installed on the test stand will differ in its actual performance from the predicted performance by the

building tolerances. Building tolerances are entirely the responsibility of the manufacturer.

Test uncertainties, on the other hand, are an expression of the uncertainty of the measuring and testing process. For example, a machine tested with 84 percent efficiency may have an actual efficiency somewhere between 82 percent and 86 percent, assuming 2 percent test uncertainties.

The test uncertainty is basically a measurement of the quality of the test. An increased test uncertainty increases the risk of failing the test if the turbomachinery is actually performing better than the acceptance level, but it reduces the risk of failing if the turbomachinery performance is lower than the acceptance level. Because it is normal practice to use a lower performance than predicted as an acceptance criterion, it is in the interest of the manufacturer as well as the user to test as accurately as possible (Figure 8).

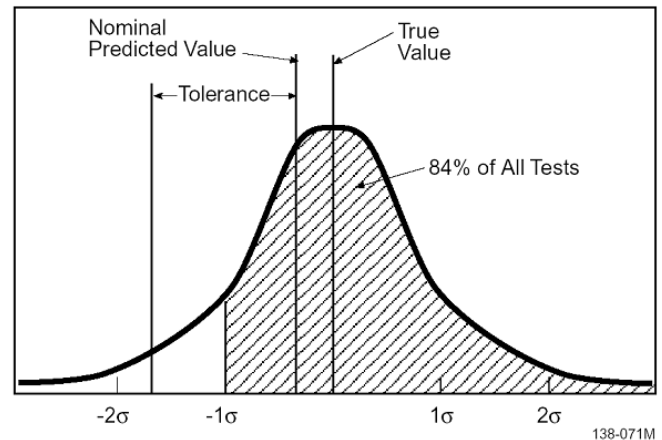


Figure 8. Test Uncertainty and Performance Tolerance.

Test uncertainties are caused by the following factors:

- Instrument accuracy and calibration
- Instrument location and installation
- Number of instruments
- Reading errors
- Unstable process

When considering instrumentation tolerances, the whole measuring chain needs to be taken into account. The instrument, such as the resistance temperature detector (RTD), thermocouple, or pressure transducer, has a certain accuracy and a certain quality of calibration. However, the overall error is also influenced by the location of the instrument (flow measurements with insufficient straight runs), the way the instrument is installed (thermocouples in thermowells without heat conductive paste or insufficient immersion depth), potential reading errors (especially if gauges are used), or the accuracy of the digital voltmeter, and the calibration quality. The following are typical instrumentation tolerances:

- Pressure 0.5 to 2.0 percent
- Temperature 0.5 to 4°F
- Flow 0.5 to 2.0 percent
- Gas composition 1.0 to 5.0 percent
- Torque 1.0 to 1.5 percent
- Equation of state 0.2 to 2.5 percent

Further, if the process shows fluctuations, it will influence the accuracy of the test results.

The use of package instrumentation leads to a considerably lower accuracy compared to tests with dedicated test instrumentation, especially due to higher calibration standards for the test instrumentation.

Package instrumentation is normally selected to allow for sufficient accuracy for trending. For trending purposes, the absolute accuracy of a measurement is not important, but rather the difference from certain baselines. Package displays usually do not take changes in gas composition into account. Furthermore, dedicated test instrumentation is calibrated on a regular basis and maintained continuously.

It is good practice to perform an uncertainty calculation to determine what possible conclusions can be drawn from the test data.

For the uncertainty analysis, it is assumed that all measurement parameters can be considered to be independent and that parameters have associated statistical bounds, such as a 95 percent confidence interval (Δu), rather than absolute limits of errors. All parameters also are assumed to have Gaussian normal distributions around their respective mean values, such that the uncertainties can be properly combined using the root-square sum method. The total uncertainty (ΔF) for a given function, $F = f(u_1, u_2, \dots, u_n)$ is, thus, determined from:

$$\Delta F = \sqrt{\left(\Delta u_1 \frac{\partial f}{\partial u_1} \right)^2 + \left(\Delta u_2 \frac{\partial f}{\partial u_2} \right)^2 + \dots + \left(\Delta u_n \frac{\partial f}{\partial u_n} \right)^2} \quad (20)$$

For this method, the overall uncertainty (ΔF) has the same statistical meaning as the individual uncertainties (Δu). Namely, if Δu represents a 95 percent confidence, then the result for the total uncertainty (ΔF) is also a 95 percent confidence interval.

While many test procedures use the rigorous application of Equation (20) to determine the uncertainty of test results, the method has its limitations: for complex relationships (e.g., when equations of state have to be considered) the equation above is rather difficult to use because the partial derivatives of all variables are not easy to obtain.

An elegant way out is the following (Moffat, 1988). If a data reduction program exists (e.g., a program that calculates compressor shaft power from flow, pressure, and temperature measurements), then the same program can be used to estimate the uncertainty in the result. This is accomplished by sequentially perturbing the input values by their respective uncertainties and recording their effects. Any term in Equation (20) can be approximated (assuming that the error is relatively small) by:

$$\left(\Delta u_1 \frac{\partial f}{\partial u_1} \right) \cong f(u_1 + \Delta u_1) - f(u_1) \quad (21)$$

That means, that the contribution of the variable u1 to the uncertainty in f can be found by calculating f twice: once with the observed value of u1 and once for u1 + Δu1 and then subtracting the two values of f. When several variables are involved, the overall uncertainty can be found by sequentially perturbing the individual variables (u1) and then finding the square root sum of the squares of the individual terms. This can be done on a spreadsheet.

To illustrate the aforementioned, the uncertainty for the compressor head, flow, efficiency, and power is demonstrated in Table 1. The first column lists the measured parameters (SG, k50, k300, pcp, and pct define the gas composition). All measured parameters have their respective test uncertainties listed in column 3. The respective readings from the instruments (averaged in the case of multiple instruments for the same parameter) are listed in column 4. The following columns are each for one of the parameters in column 1, and only that parameter is perturbed by the test uncertainty for this parameter. For example, column 6 (for the discharge pressure p2) changes only the value for p2 by its test uncertainty (0.25 percent), and leaves all the other parameters as in column 4 [Equation (21)]. For each column, the values for head, flow efficiency, and power are calculated and compared to the nominal values from the data in column 4. The absolute test uncertainty is then the square root of the sum of the differences squared [Equation (20)].

Table 1. Spreadsheet for Test Uncertainty Calculation.

Parameter	Units	Uncertainty	Nominal Value	P1	P2	T1	T2	P_flow	T_flow	DP	DP Off	Rpe	Id	Orifice Id	SG	k50	k300	pcp	pct
F1	hp	0.2%	726.66	730.30	726.64	726.96	726.46	726.96	726.66	726.66	726.66	726.66	726.66	726.66	726.66	726.66	726.66	726.66	726.66
T2	psia	0.2%	1202.73	1202.73	1202.73	1202.73	1202.73	1202.73	1202.73	1202.73	1202.73	1202.73	1202.73	1202.73	1202.73	1202.73	1202.73	1202.73	1202.73
F_flow	psia	0.2%	726.66	726.66	726.66	726.66	726.66	726.66	726.66	726.66	726.66	726.66	726.66	726.66	726.66	726.66	726.66	726.66	726.66
T_flow	psia	0.2%	1202.73	1202.73	1202.73	1202.73	1202.73	1202.73	1202.73	1202.73	1202.73	1202.73	1202.73	1202.73	1202.73	1202.73	1202.73	1202.73	1202.73
DP Off	psia	0.2%	603.00	603.00	603.00	603.00	603.00	603.00	603.00	603.00	603.00	603.00	603.00	603.00	603.00	603.00	603.00	603.00	603.00
Pipe ID	in	0.002	10.500	10.500	10.500	10.500	10.500	10.500	10.500	10.500	10.500	10.500	10.500	10.500	10.500	10.500	10.500	10.500	10.500
Orifice D	in	0.002	7.944	7.944	7.944	7.944	7.944	7.944	7.944	7.944	7.944	7.944	7.944	7.944	7.944	7.944	7.944	7.944	7.944
SG		0.002	0.002	0.002	0.002	0.002	0.002	0.002	0.002	0.002	0.002	0.002	0.002	0.002	0.002	0.002	0.002	0.002	0.002
k50		0.002	1.280	1.280	1.280	1.280	1.280	1.280	1.280	1.280	1.280	1.280	1.280	1.280	1.280	1.280	1.280	1.280	1.280
k300		0.002	1.280	1.280	1.280	1.280	1.280	1.280	1.280	1.280	1.280	1.280	1.280	1.280	1.280	1.280	1.280	1.280	1.280
pcp	psia	0.002	671.10	671.10	671.10	671.10	671.10	671.10	671.10	671.10	671.10	671.10	671.10	671.10	671.10	671.10	671.10	671.10	671.10
pct	psia	0.002	303.00	303.00	303.00	303.00	303.00	303.00	303.00	303.00	303.00	303.00	303.00	303.00	303.00	303.00	303.00	303.00	303.00
C-head		0.003	0.003	0.003	0.003	0.003	0.003	0.003	0.003	0.003	0.003	0.003	0.003	0.003	0.003	0.003	0.003	0.003	0.003
Z1		0.003	0.003	0.003	0.003	0.003	0.003	0.003	0.003	0.003	0.003	0.003	0.003	0.003	0.003	0.003	0.003	0.003	0.003
Z2		0.003	0.003	0.003	0.003	0.003	0.003	0.003	0.003	0.003	0.003	0.003	0.003	0.003	0.003	0.003	0.003	0.003	0.003
W		14073.6	14073.6	14073.6	14073.6	14073.6	14073.6	14073.6	14073.6	14073.6	14073.6	14073.6	14073.6	14073.6	14073.6	14073.6	14073.6	14073.6	14073.6
η		0.008	0.008	0.008	0.008	0.008	0.008	0.008	0.008	0.008	0.008	0.008	0.008	0.008	0.008	0.008	0.008	0.008	0.008
Y		0.008	0.008	0.008	0.008	0.008	0.008	0.008	0.008	0.008	0.008	0.008	0.008	0.008	0.008	0.008	0.008	0.008	0.008
Standard Flow	mass/hr	269.43	269.43	269.43	269.43	269.43	269.43	269.43	269.43	269.43	269.43	269.43	269.43	269.43	269.43	269.43	269.43	269.43	269.43
Head	ft/rev	2147	2146	2180	2178	2187	2187	2187	2187	2187	2187	2187	2187	2187	2187	2187	2187	2187	2187
Flow	psia	-0.2%	101	19	0	0	0	0	0	0	0	0	0	0	0	0	0	0	0
Efficiency	psia	1.03%																	
Power	psia	0.14%	30.326	0.226	0.2219	0.209	0.1516	0.1516	0.1516	0.1516	0.1516	0.1516	0.1516	0.1516	0.1516	0.1516	0.1516	0.1516	0.1516
Head	psia	-0.005	0.006	0.006	0.003	0.003	0.003	0.003	0.003	0.003	0.003	0.003	0.003	0.003	0.003	0.003	0.003	0.003	0.003
Flow	psia	0.002	0.002	0.002	0.002	0.002	0.002	0.002	0.002	0.002	0.002	0.002	0.002	0.002	0.002	0.002	0.002	0.002	0.002
Efficiency	psia	1.19%																	
Power	psia	0.04%																	
Head	psia	0.001	0.001	0.001	0.001	0.001	0.001	0.001	0.001	0.001	0.001	0.001	0.001	0.001	0.001	0.001	0.001	0.001	0.001
Flow	psia	-0.2%	101	19	0	0	0	0	0	0	0	0	0	0	0	0	0	0	0
Efficiency	psia	1.03%																	
Power	psia	0.14%																	
Head	psia	-0.005	0.006	0.006	0.003	0.003	0.003	0.003	0.003	0.003	0.003	0.003	0.003	0.003	0.003	0.003	0.003	0.003	0.003
Flow	psia	0.002	0.002	0.002	0.002	0.002	0.002	0.002	0.002	0.002	0.002	0.002	0.002	0.002	0.002	0.002	0.002	0.002	0.002
Efficiency	psia	1.19%																	
Power	psia	0.04%																	
Head	psia	0.001	0.001	0.001	0.001	0.001	0.001	0.001	0.001	0.001	0.001	0.001	0.001	0.001	0.001	0.001	0.001	0.001	0.001
Flow	psia	-0.2%	101	19	0	0	0	0	0	0	0	0	0	0	0	0	0	0	0
Efficiency	psia	1.03%																	
Power	psia	0.14%																	
Head	psia	-0.005	0.006	0.006	0.003	0.003	0.003	0.003	0.003	0.003	0.003	0.003	0.003	0.003	0.003	0.003	0.003	0.003	0.003
Flow	psia	0.002	0.002	0.002	0.002	0.002	0.002	0.002	0.002	0.002	0.002	0.002	0.002	0.002	0.002	0.002	0.002	0.002	0.002
Efficiency	psia	1.19%																	
Power	psia	0.04%																	

For example, the absolute uncertainty for power is 220 hp, which amounts to 2.87 percent of the nominal value. In the example, it also becomes immediately obvious that the largest contributor to the uncertainty of the absorbed power is the inaccurate measurement of the pipe inner diameter, while the (in this case very accurate) measurements of temperature and pressure at suction and discharge are the key contributors to the accuracy of the efficiency measurement.

The beauty of this scheme lies in the fact that:

- It does not matter whether the uncertainty is given as an absolute or relative number.
- The procedure can be implemented using any of the commercial spreadsheet programs.
- Any value in the table can be the result of a complex, even iterative, calculation.

More details on test uncertainty calculation can be found in Moffat (1988), ASME PTC 19.1 (1985), Kurz, et al. (1999), and Kurz (2001).

INTERPRETATION OF TEST DATA

If the test data deviate from the predictions or from other test data by more than the level of test uncertainty, the reasons must be explored. Assuming the test data are reduced correctly, it must be determined whether the test conditions were close enough to the conditions for the prediction.

It is usually desirable to use redundant data for comparison. Examples follow.

Determine the shape of the head-flow and flow efficiency curves, and compare them with predictions. If the curves are just shifted to the left or right, the flow measurement is suspect. Another necessary step is to compare the whole measured φ-ψ-η curve with the predicted curve. For compressors, it might be found that the head-versus-flow curves have just shifted horizontally, which points to an incorrect flow measurement. If some points of the curve match the predictions and others do not match, variations of the gas composition during the test could be the cause. Data from a site test (Figure 9) for a compressor station close to several wells serves as an example. The solid line represents the prediction for head and efficiency. The symbols indicate test data taken during two tests. Test 1 experienced significant fluctuations in gas composition, while test 2 was somewhat more stable.

Additional evidence may come from a comparison between compressor absorbed power and expected driver available power:

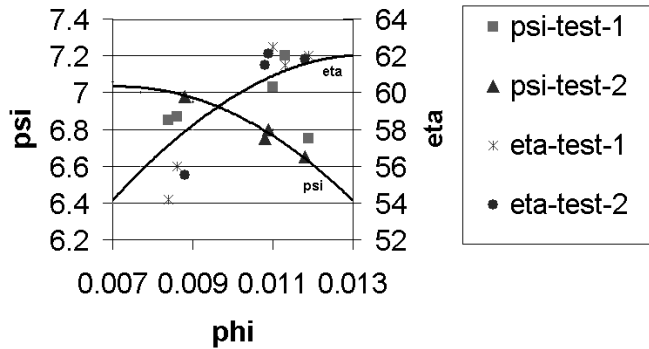


Figure 9. Data Scatter Due to Unstable Gas Composition—Test 1 Experienced Fluctuations in the Gas Composition. Test 2, on the Same Compressor, Was More Stable.

determine the absorbed power and compare it with the expected power from the driver. For a gas turbine, full load factory test data are usually available. The compressor should be operated at a point that requires the gas turbine to operate at full load. The absorbed compressor power should be close to the as-factory-tested gas turbine power (corrected to the site test conditions regarding ambient conditions and power turbine speed), assuming the gas turbine is in new and clean condition. For electric motor driven compressors, the motor, gearbox, and variable frequency drive (VFD) efficiencies can be used to compare the measured electric power consumption to the absorbed compressor power.

Head and efficiency low—a comparison to available other test data should be made. If the head was already low in a factory test, then the results from the site test may just confirm the factory test findings. A wrong flow measurement can make the compressor look like it is not producing the correct head and efficiency (refer above). Other reasons include damaged impellers or damaged seals. Both issues can be eliminated by visual inspection, if possible. Damaged balance piston seals can also be detected by monitoring the pressure (or flow) in the balance piston return line. Ingested inlet strainers that are caught in the inlet (or other obstructions) cause significant pressure drop between the measurement location and the actual compressor inlet, thus generating the impression that compressor is low in head and efficiency.

Any data taken must be corrected to the same datum conditions. For gas compressors, the nondimensional curves are a good tool. However, large deviations in Mach number (Figure 7), especially in multistage machines, need to be avoided.

On gas compressors, the effects of different Mach numbers or different volume/flow ratios (Q_s/Q_d) may be responsible for the deviations. In such cases, it is always helpful to repeat the prediction procedure for the actual test conditions.

In many instances, redundant measurement can increase the confidence in the results. The compressor gas power can be checked by comparing the results with the gas turbine power and heat rate from the factory test, corrected to site test conditions (Kurz, 1999). In this case, it is also recommended to thoroughly clean the gas turbine air compressor prior to the test; 3 percent and more engine power have been recovered after cleaning the air compressor. Electric motors allow a convenient measurement of the electric power input. Corrected by the motor efficiency, the gearbox efficiency, the losses in the variable frequency drive (if applicable), the motor shaft power can be calculated and compared to the measured compressor power.

It is good practice to perform a test uncertainty calculation as part of the data evaluation. Obviously, data with an uncertainty of 3 percent cannot yield conclusions that require an accuracy of 1 percent. If the test point does not match the prediction or other test results, a test uncertainty ellipse (Figure 10) can be drawn. The two axes of the ellipse represent the test uncertainties for the parameters on the x and y axis, respectively. If it still covers the prediction,

the test results might be correct. The uncertainty ellipse in Figure 10 expresses the fact that not only is the measured head subject to test uncertainties, but also the measured flow. When comparing field test results with factory tests, the influence of test uncertainties in both tests must be considered. Whatever factory test results are available, they can be used for comparison and verification purposes. Whatever the deviation might be, it is best if it can be detected, discussed, and possibly corrected during the test. A good relationship with a trusted manufacturer can help in finding causes for discrepancies.

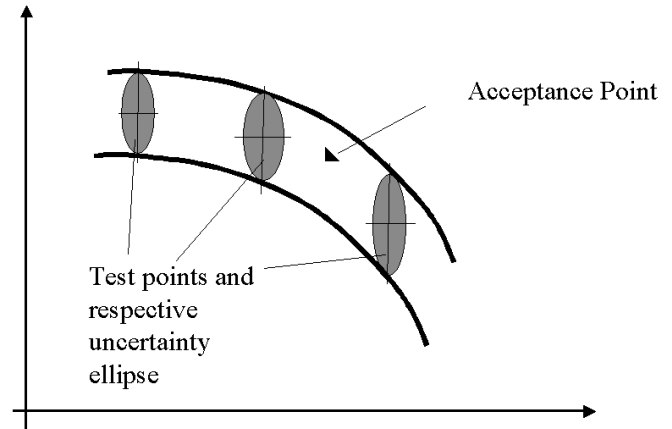


Figure 10. Comparison of Multiple Test Points, Their Respective Test Uncertainties, with the Acceptance Point.

Another reason for test data discrepancies can be found in the way the test is conducted. If the test data have not been taken while the equipment operated under steady-state conditions, they may not be useful. Before readings are taken for any individual test point, steady-state operating conditions must be achieved. Steady-state is achieved if all of the following apply during the 10-minute interval.

- Operating speed constant within 5 rpm
- Fluctuations of the efficiency reading no larger than ± 0.5 points from average, while head and actual flow remain within ± 0.5 percent from average, respectively.

The driving gas turbine (where applicable) must be heat soaked if the compressor test point requires full load, to avoid drift. The time requirement to achieve heat soaking should be provided by the gas turbine manufacturer. As a rule of thumb, one hour is required for smaller engines (below, say 8000 hp), while larger engines may require two or more hours. A well conducted test will yield repeatable and reliable results. In Figure 11, the results of several tests at two different stations, including data for four identical compressors, tested consecutively, can serve as proof for this statement.

CONCLUSIONS

Based on the information provided in this paper, the test engineer can convert raw test data into meaningful data that can be used for evaluating the performance of a gas turbine or a gas compressor. The data reduction was explained based on the basic relationships of pressure, temperature, flow, and head, as well as the operational characteristics of gas turbines and centrifugal gas compressors. The appropriate use of performance maps was explained.

NOMENCLATURE

- c_p = Specific heat at constant pressure
- C = Discharge coefficient
- E = Velocity approach factor

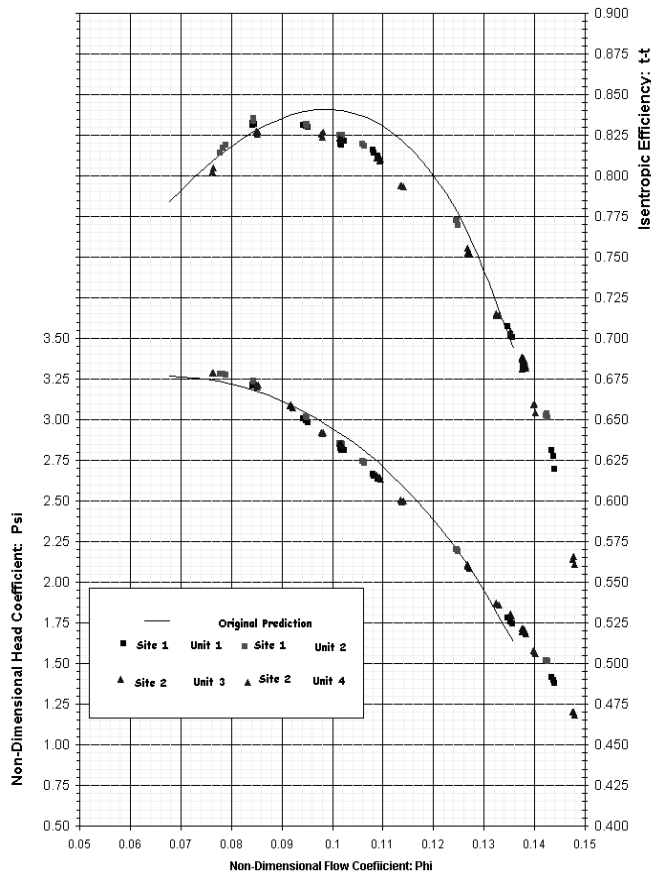


Figure 11. Site Test Results for Four Aerodynamically Identical Compressors at Two Different Sites.

- EOS = Equation of state
- BWRS = Benedict-Webb-Rubin-Starling
- LKP = Lee-Kesler-Ploecker
- PR = Peng-Robinson
- RK = Redlich-Kwong
- SRK = Soave-Redlich-Kwong
- f = Function
- h = Enthalpy
- H = Head
- HR = Heat rate
- k = Isentropic exponent
- LHV = Lower heating value
- Ma = Mach number
- MW = Molecular weight
- N = Speed (s^{-1})
- p = Pressure
- P = Power
- Q = Volumetric flow
- R = Gas constant
- Re = Reynolds number
- SQ = Standard flow
- T = Temperature
- u = Function variable
- u = Velocity of the impeller tip
- v = Specific volume
- W = Mass flow
- Z = Compressibility factor
- ρ = Density
- π = Torque
- η = Efficiency
- φ = Flow coefficient
- ψ = Head coefficient

Subscripts

- a = Acceptance
- amb = Ambient
- d = Compressor discharge nozzle
- GB = Gearbox
- I = Inlet
- L = Leakage
- M = Mechanical
- packg = Package
- s = Compressor suction nozzle
- SL = Sea level
- t = Test
- tip = Impeller tip

Superscripts

- * = Isentropic
- p = Polytopic
- I = Section I

REFERENCES

ASME PTC 10, 1997, "Compressors and Exhausters," American Society of Mechanical Engineers, New York, New York.

ASME PTC 19.1, 1985, "Measurement Uncertainties," American Society of Mechanical Engineers, New York, New York.

ASME PTC 19.5, 1971, "Fluid Meters," American Society of Mechanical Engineers, New York, New York.

Baehr, H. D., 1981, *Thermodynamik*, Berlin, Germany: Springer.

Beinecke, D. and Luedtke, K., 1983, "Die Auslegung von Turboverdichtern unter Beruecksichtigung des realen Gasverhaltens," VDI Berichte, (487), pp. 271-279.

Brown, R.N., 1991, "Fan Laws, the Use and Limits in Predicting Centrifugal Compressor Off Design Performance," *Proceedings of the Twentieth Turbomachinery Symposium*, Turbomachinery Laboratory, Texas A&M University, College Station, Texas, pp. 91-100.

ISO 5167, 1980, "Measurement of Fluid Flow by Means of Orifice Plates, Nozzles and Venturi Tubes Inserted in Circular Cross-Section Conduits Running Full," International Organization for Standardization, Geneva, Switzerland.

Kumar, S. K., Kurz, R., O'Connell, J. P., 1999, "Equations of State for Compressor Design and Testing," ASME Paper 99-GT-12.

Kurz, R., Brun, K., Legrand, D.D., 1999, "Field Performance Testing of Gas Turbine Driven Compressor Sets," *Proceedings of the Twenty-Eighth Turbomachinery Symposium*, Turbomachinery Laboratory, Texas A&M University, College Station, Texas, pp. 213-230.

Kurz, R., 2001, "Site Performance Testing of Gas Turbine Driven Centrifugal Compressors," GMRC Gas Machinery Conference, Austin, Texas.

Moffat, R. J., 1988, "Describing the Uncertainties in Experimental Results," *Experimental Thermal and Fluid Science*, 1:3-17.

Poling, B. E., Prausnitz, J. M. and O'Connell, J. P., 2001, *The Properties of Gases and Liquids*, Fifth Edition, New York, New York: McGraw Hill.

VDI 2045, 1993, "Acceptance and Performance Tests on Turbo Compressors and Displacement Compressors," Verein Deutscher Ingenieure e.V., Düsseldorf, Germany.

BIBLIOGRAPHY

AGA Report No 3, 1991, "Orifice Metering of Natural Gas," American Gas Association, Washington, D.C.

ASME PTC 22, 1997, "Gas Turbine Power Plants," American Society of Mechanical Engineers, New York, New York.

Kurz, R. and, Fozi, A. A., 2002, "Acceptance Criteria for Gas Compression Systems," ASME Paper GT-2002-30282.

Robinson, R. L. and Jacobi, R. H., 1965, "Better Compressibility Factors," *Hydrocarbon Processing*, 4.